ISSN 2004-2965 Energy Proceedings, Vol. 19, 2021

**International Conference on Applied Energy 2021**
**Nov. 29 - Dec. 5, 2021, Thailand/Virtual**
**Paper ID: 500**

# Structural optimization of thermoelectric generator with different circuit layouts used for exhaust heat recovery

Wei He*, Zihan Cai, Shengchun Liu, Yulin Wang, Jian Liu, Lingran Meng

Tianjin Key Laboratory of Refrigeration Technology, Tianjin University of Commerce, Tianjin 300134, PR China
*Correspondence: weihe@tjcu.edu.cn

**ABSTRACT**

To fully utilize automobile exhaust waste heat, a thermoelectric generator can be used to recover waste heat energy. In this study, an engine exhaust thermoelectric generation model based on a smooth plate-type exhaust heat exchanger is established, and the thermoelectric performance is quantified using Fortran. To achieve the maximal net power output of the thermoelectric generator, the different series circuit layouts of the thermoelectric module were compared, and the structural optimization of the exhaust heat exchanger was performed. The results show that there are optimal values for the total length, width, and height scale of the exchanger for both the full-and two-stage series circuit types. At the exhaust temperature of 500 °C and mass flow rate of 30 g $s^{-1}$, the optimal exchanger heights of the full-and two-stage series types are both 4 mm, and the optimal number of thermoelectric units $N_{y,opt}$ in the *y* direction is 68 pairs. The optimal number of thermoelectric units $N_{x,opt}$ in the *x-direction* is 44 pairs for the full series type and 54 pairs for the two-stage series type. When the corresponding optimal scales are utilized, the two-stage series type increases by 11.39 % compared with the full-series type.

**Keywords:** circuit layout; optimal structure, thermoelectric generation; output power, exhaust

## 1. INTRODUCTION

Owing to the limitations of the existing energy resources, new power generation technologies have been widely studied and are expected to replace the green technology of fuel-based energy [1]. Semiconductor thermoelectric generation is a technology that directly converts thermal energy into electrical energy based on the Seebeck effect of thermoelectric materials. It is advantageous given its all-solid-state energy conversion mode that results in the absence of pollution, noise, or moving parts, and it is highly reliable. However, due to its relatively low thermoelectric conversion efficiency, it is not widely used, and researches are being conducted on ways to increase the power output of these generators [2].

In recent years, many scholars have conducted studies on thermoelectric materials and structural optimization. Thermoelectric materials have significantly improved performance indicators [3 – 4]. However, optimizing the module structure via high-performance thermoelectric materials is an effective way to improve the output power of thermoelectric generators. Before developing the actual thermoelectric generator products, an analysis of the performance of thermoelectric generators through numerical simulation is normally required. Moreover, it is necessary to design or optimize the thermoelectric module structure for achieving the highest conversion efficiency [5]. In terms of optimizing the structure of thermoelectric modules, many studies based on numerical models have been published. For instance, Meng [6] proposed a spiral thermoelectric structure and compared the voltage, current, power, and efficiency of the spiral module and the straight module with the change in temperature difference. The influence of module spacing on the thermoelectric performance was scrutinized. Moreover, the changes in the unit input heat and unit output power with logarithms and directs were analyzed as well. Their results showed that as the conversion efficiencies of the two modules are roughly equal, the spiral module can obtain more heat than the straight module, yielding a higher output power. Shu [7] chose the output power as the optimization goal and compared the performance of thermoelectric modules with two different structures and configurations. In the single thermoelectric module mode, the segmented structure was used to match the radial large temperature gradient, and the maximum output power was increased (i.e. improved) by 13.4 % compared with the original mode. The TEG (thermoelectric generator) system with multiple thermoelectric modes exhibited good results for waste heat recovery. Installing straight fins along the flow direction can improve the heat transfer intensity and reduce the thermal resistance. The radiator should be arranged at a lower temperature to improve the temperature uniformity and output power. Cheng [8] compared the maximum power density and conversion efficiency of a single-stage and two-stage TEG. The results showed that the single-stage TEG had the advantage of maximum power density, and the two-stage TEG had a higher conversion efficiency at the same inlet temperature. Both the maximum power density and the corresponding conversion efficiency increase with an increase in the inlet temperature. At the same time, the two-stage configuration can improve the conversion efficiency by reducing the heat conduction from the heating channel to the cooling channel. Jang [9] and Favarel [10] analyzed the influence of thermoelectric module spacing (or occupancy rate) placed on a fixed geometry heat exchanger on the thermoelectric performance. They showed that the maximum output power can be achieved by optimizing the spacing. Thus, many important research results have been achieved in the optimization of thermoelectric modules. However, it should be noted that the current structural optimization of the thermoelectric module was mainly aimed at the structure of the thermoelectric arms and the spacing of the thermoelectric arms of the traditional thermoelectric model, and the structural optimization of the segmented layout connection mode is still lacking. To this end, this study estimates the effect of different circuit layout connection modes on the thermoelectric performance and performs structural optimization by taking the net power output as the research goal.

## 2. THERMOELECTRIC MODEL

### *2.1 Model description*

The overall structure of the exhaust TEG is illustrated in Fig. 1. The exhaust heat exchanger was placed between the two thermo–electric modules and served as the heat source. The cooling water heat exchanger channel was arranged on the other side of the thermoelectric module as the cold source of the thermoelectric module.

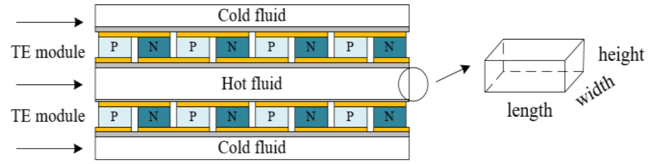


Fig. 1 Overall structure of thermoelectric generator

Fig. 2 shows the schematic diagram of the different series circuit layouts for the thermoelectric generator. In the figure, there are $N_x$ thermoelectric units along the $x$ direction (exhaust flow direction) and $N_y$ units in the $y$ direction (across flow direction). Along the x direction, the $N_x$ thermoelectric units were equally divided into one or two series circuits, and the number of thermoelectric units in each series block is $n_x$. Fig.2(a) shows the full series type, while Fig. 2(b) shows the two-stage series type. All the output circuits produced by the thermo–electric modules were connected to a storage battery to collect the conversion power.

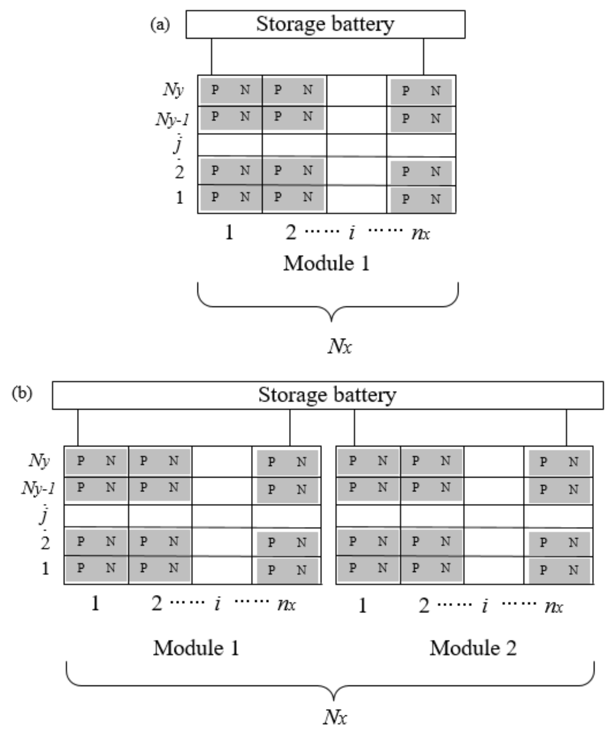


Fig. 2 Schematic diagram of series circuit layout for thermoelectric generator(a) full series type (b) two-stage series type

One thermoelectric module containing $n_x \times N_y$ PN pairs, where the coordinates $(i, j)$ represent the PN pair number of lines and rows, with $i = 1$ to $n_x$, and $j = 1$ to $N_y$. Assuming *that* $N_y$ PN couples contained in a row have the same temperature characteristics, the heat transfer equilibrium equations for the $i_{th}$ thermoelectric element can be described according to [11] as shown in Eq. 1 and 2 below:

$$q_h^i = 0.5c_f m_f (T_f^i - T_f^{i+1}) = n_y \left[ \alpha_{pn} I T_h^i + K_{pn}(T_h^i - T_L^i) - 0.5 I^2 R_{pn} \right] = n_y ab \left[ 0.5\left(T_f^i + T_f^{i+1}\right) - T_h^i \right] / \left(R_{f1} + R_{f2} + R_{f3}\right) \quad (1)$$

$$q_L^i = 0.5c_c m_c (T_c^{i+1} - T_c^i) = n_y \left[ \alpha_{pn} I T_L^i + K_{pn}(T_h^i - T_L^i) + 0.5 I^2 R_{pn} \right] = n_y ab \left[ 0.5\left(T_c^i + T_c^{i+1}\right) - T_h^i \right] / \left(R_{c1} + R_{c2} + R_{c3}\right) \quad (2)$$

where $q_h^i$ is the amount of heat released by the hot fluid to the hot end of the thermoelectric module, $q_L^i$ is the amount of heat released from the surface of the cold end of the thermoelectric module to the cold fluid, *and* $T_f^i$ and $T_c^i$ are the temperatures of the hot and cold fluids of the thermoelectric units, respectively. The thermal fluid temperature of the ith thermoelectric unit decreased from $T_f^i$ to $T_f^{i+1}$. The cold fluid temperature of the ith thermoelectric unit increased from $T_c^{i+1}$ to $T_c^i$. where $c_f$ and $c_c$ are the specific heat capacities of the hot and cold fluids, respectively; $m_f$ and $m_c$ are the total mass flow rates of the hot and cold fluids, respectively; $\alpha_{pn}$ denotes the Seebeck coefficient, $K_{pn}$ represents the thermal conductance, and $R_{pn}$ indicates the electric resistance for a P–N semiconductor couple.

These can be obtained as shown in Eqs. 3, 4, and 5 below:

$$\alpha_{pn} = \alpha_p - \alpha_n \quad (3)$$

$$K_{pn} = c_1 c_2 (\lambda_p + \lambda_n) / c_3 \quad (4)$$

$$R_{pn} = c_3 (\rho_p + \rho_n) / (c_1 c_2) , \quad (5)$$

where $\alpha_p$, $\rho_p$, $\lambda_p$, $\alpha_n$, $\rho_n$, and $\lambda_n$ are the Seebeck coefficient, resistivity, and thermal conductivity, respectively, of the P-type and N-type legs, *and* $c_1$, $c_2$, *and* $c_3$ are the length, width, and height of the semiconductor leg, respectively, for both the P- and N-type exchangers.

The total thermoelectric power output for one module is formalized by Eq. 6:

$$P_{teg} = 2\sum_{i=1}^{n_x} \left(q_h^i - q_L^i\right) \quad (6)$$

Pump power consumed given the flow resistance when exhaust gas flows through the passage [12] is formalized according to Eq. 7:

$$P_{pump} = f_z (m_f / \rho_f) \quad (7)$$

where $f_z$ is the pressure drop of the heat exchanger at the overheated end of the tail flow, and $\rho_f$ is the density of the exhaust gas fluid.

Therefore, the net output power of the thermoelectric system is

$$P_{net} = P_{teg} - P_{pump} \quad (8)$$

When the thermal fluid flows through the TEG, the temperature continuously decreases, and its physical parameters are also modified. Here, the physical properties of air are used as the physical parameters of the thermal fluid. The basic calculation parameters of the thermoelectric system are shown in Table 1. Note that the HZ-20 commercial thermoelectric module was selected for analysis, and the physical parameters of the thermoelectric materials are shown in Table 2.

Table 1 Basic calculation parameters of thermoelectric system

| Item | Value | Item | Value |
|---|---|---|---|
| $c_1$(m) | 0.005 | $m_f$(g s$^{-1}$) | 30 |
| $c_2$(m) | 0.005 | $m_c$(g s$^{-1}$) | 426 |
| $c_3$(m) | 0.003 | $T_c^1$(°C) | 71 |
| $h_c$(W m$^{-2}$ K$^{-1}$) | 1000 | $T_f^1$(°C) | 500 |
| $\alpha_P$(V K$^{-1}$) | 2.037×10$^{-4}$ | $\alpha_N$(V K$^{-1}$) | -1.721×10$^{-4}$ |
| $\rho_p$ (S m$^{-1}$) | 1.314×10$^{-5}$ | $\rho_n$ (S m$^{-1}$) | 1.119×10$^{-5}$ |
| $\lambda_p$ (W m$^{-1}$ K$^{-1}$) | 1.265 | $\lambda_n$ (W m$^{-1}$ K$^{-1}$) | 1.011 |

### *2.2 Model validation*

A comparison between the simulation and experimental results (Fig. 3) is shown to validate the robustness of the calculation results of the established mathematical model. The calculation results obtained by this program were compared with the experimental data from the literature [13]. In the experiment, a heater with a heating area of 40 mm$^2$ was set at the hot end of the thermoelectric module, and the test heat flows $Q_h$ were 10, 20, 30, 40, and 50 W, respectively. The type of thermoelectric module selected in the test was teg1-127-1.4-1.6, the structural size was 40 mm × 40 mm × 3.8 mm, and the cooling mode was water cooling. In the simulation calculation, thermoelectric conditions and physical parameters, similar to those in the literature, were adopted to quantify the thermoelectric output power under different heat flows. The bias between the simulated calculation results and the experimental results is < 2% according to the comparison. Thus, the accuracy of the model, established in this study and the self-written calculation program, is validated.

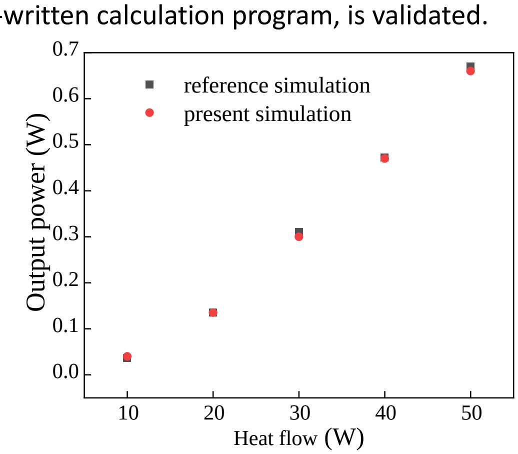


 

Fig. 3 Comparison between simulation results and experimental results

## 3. RESULTS AND DISCUSSION

Fig. 4 shows the change in the net power with the thermoelectric unit number along *the* x-direction $N_x$ when the thermoelectric unit number along the *y* direction $N_y$ is 60 pairs for the case when the exhaust heat exchanger height is 5 mm. As seen, when the heat exchanger height and width are fixed, with the increase of $N_x$, the net power increases first and then decreases regardless the type of series (the full series or the two-stage series). There exists an optimal number of thermoelectric units along the *x-direction*, which is $N_{x,opt}$ = 55 for the full series type and $N_{x,opt}$ = 68 for the two-stage series type, where the net power reaches the peak. Also, the obtained maximal net power of the two-stage series type was significantly higher than that of the full series type.

Fig. 5 shows that $N_{x,opt}$ varies with the $N_y$ number for different numbers of segments for a fixed channel height of 5 mm. It is therefore evident that with the increase in $N_y$, the optimal number of thermoelectric elements along the *x-direction* $N_{x,opt}$ is nearly stable for both types of circuit connection types. Therefore, $N_y$ has insignificant effect on the optimal number of thermoelectric elements along the *x-direction* $N_{x,opt}$.

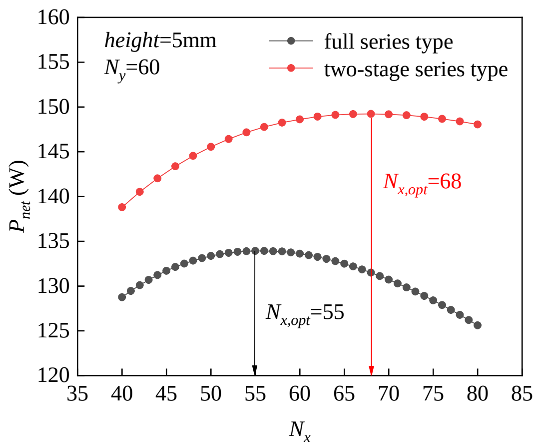


Fig. 4 Variations of net power with $N_x$ at different number of sections

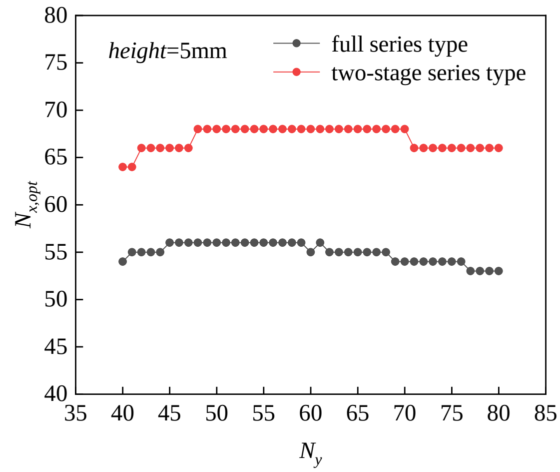


Fig. 5 Changes of $N_{x,opt}$ with $N_y$ in different segment numbers

Based on Fig. 5, the change in the corresponding net power with $N_y$ is shown in Fig. 6. This indicates on an optimal number of thermoelectric units along the *y* direction $N_{y,opt}$ to make the net power reach the peak for both circuit connection types. The optimal number of $N_{y,opt}$ is the same for both types, that is, $N_{y,opt}$ = 55. Therefore, when the channel height is fixed, with net power as the goal, the thermoelectric module has the optimal total length and total width regardless the type of series as well (full series or two-stage series). However, if the optimal scales are considered, the net power of the two-stage series type is higher than that of the full series type.

Fig. 7 demonstrates the variation of $N_{x,opt}$ and $N_{y,opt}$ with different circuit connection types for different heat exchanger heights. It is seen that with the increase in the heat exchanger height, $N_{y,opt}$ gradually, but nonlinearly decreases, while $N_{x,opt}$ gradually and linearly increases. For any given height, $N_{x,opt}$ for the two-stage series type is higher than the series type, but $N_{y,opt}$ is the same for the both circuit types.

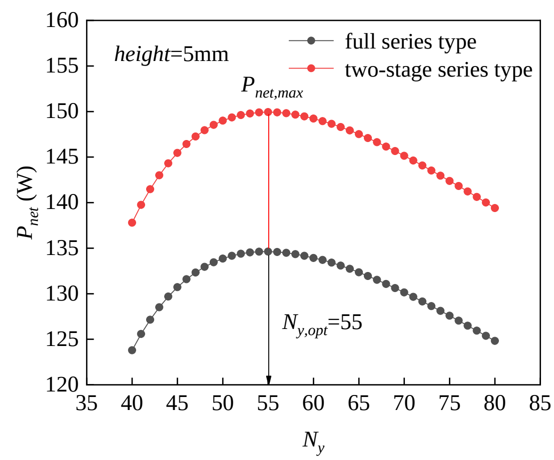


Fig. 6 Change of net power with $N_y$ at different number of sections

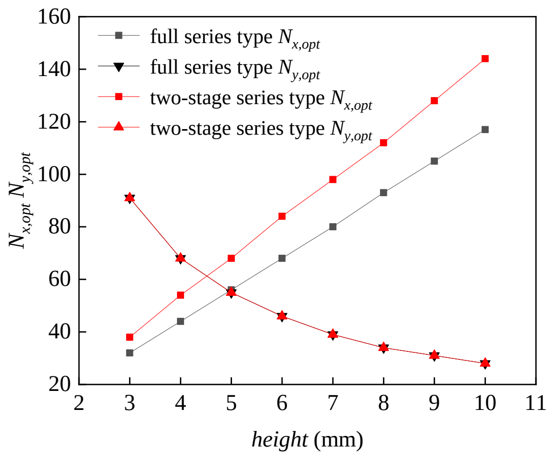


Fig. 7 Optimum length width varies with channel height under different circuit connection modes

When the optimal scales are taken, as shown in Fig. 7, the corresponding maximal power outputs are as shown in Fig. 8. The output performance of the two-stage series type was significantly superior than that of the full series type. The results show that there are optimal values for the total length, width, and height scale of the exchanger for both the full-and two-stage series circuit types. As the height increases, the power decreases. Considering manufacturing issues, the optimal height is 4 mm for both the full series type and the two-stage series type in this case. At the optimal height of 4 mm, the maximum net output power of the full series type is 135.54 W, and that of the two-stage series type is 150.98 W. Overall, the output power of the two-stage series type increased by 11.39 % compared with the full series type.

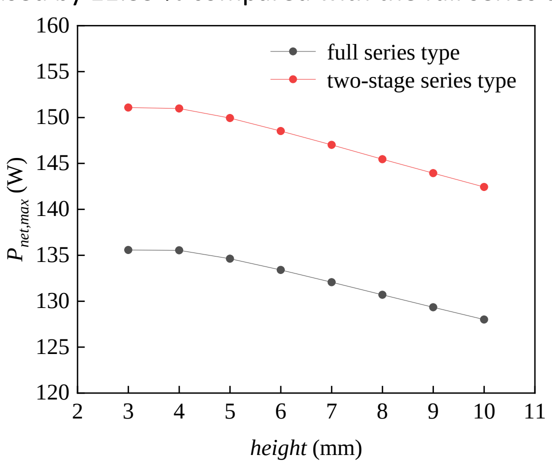


Fig. 8 The optimal net power varies with channel height under different circuit connection modes

## 3. CONCLUSIONS

In this study, the exhaust temperature and exhaust mass flow rate were taken as 500 °C and 30 g s$^{-1}$, respectively. Taking the maximum net power as the goal, the structure of the exhaust heat exchanger with different circuit layout connections was optimized, and the following conclusions were deduced.

First, at a constant height of the exhaust heat exchanger, there are optimal lengths and widths. The optimal length for the two-stage series type is higher than that of the series type, but the optimal width is the same for both circuit types. Moreover, an optimal height exists and can be determined. The analysis of the full series circuit and two-stage series circuit type showed that they have the same optimal height of 4 mm and the same optimal $N_{y,opt}$=68 pairs. However, they had different values of optimal $N_{x,opt}$; $N_{x,opt}$ = 44 pairs for the full series type and $N_{x,opt}$ = 54 pairs for the two-stage series type.

Second, under the same conditions, the power output of the two-stage series type was substantially better than that of the full series type. When the optimal height of 4 mm is taken, the net output power of full series type is 135.54 W, and the of the two-stage series type is 150.98 W. The intercomparison between them indicates that the power of the two-stage series type increases by 11.39 %.


## ACKNOWLEDGEMENTS

The authors are grateful for financial support from the National Natural Science Foundation of China (51806152), the International Cooperation Program of the Ministry of Science and Technology of China (2017YFE0198000), and the Tianjin Natural Science Foundation (No.18JCZDJC97100).


## REFERENCE


[1] Basel I. Ismail, Wael H. Ahmed. Thermoelectric Power Generation Using Waste-Heat Energy as an Alternative Green Technology. Recent Patents on Electrical Engineering. 2009; 2(1) .

[2] Liang G, Zhou J, Huang X. Analytical model of parallel thermoelectric generator. Applied Energy, 2011, 88(12):5193-5199.

[3] Zhu T J. Research progress of thermoelectric materials and devices. Journal of inorganic materials, 2019, 34(03):3-5.

[4] Alam H, Ramakrishna S. A review on the enhancement of figure of merit from bulk to nano-thermoelectric materials. Nano Energy, 2013, 2(2):190-212.

[5] BjøRk R, Christensen D V, Eriksen D, et al. Analysis of the internal heat losses in a thermoelectric generator. International Journal of Thermal Sciences, 2014, 85:12-

20.
[6] Meng X, Suzuki R O. Helical configuration for thermoelectric generation. Applied Thermal Engineering, 2016, 99:352-357.
[7] Shu G, Ma X, Hua T, et al. Configuration optimization of the segmented modules in an exhaust-based thermoelectric generator for engine waste heat recovery. Energy 2018:S0360544218312404-.
[8] Cheng K, Zhang D, Qin J, et al. Performance evaluation and comparison of electricity generation systems based on single- and two-stage thermoelectric generator for hypersonic vehicles. Acta Astronautica, 2018:S0094576517315977.
[9] Jang J-Y, Tsai Y-C. Optimization of thermoelectric generator module spacing and spreader thickness used in a waste heat recovery system. Applied Thermal Engineering 2013;51:677–89.
[10] Favarel C, Bédécarrats J-P, Kousksou T, et al. Numerical optimization of the occupancy rate of thermoelectric generators to produce the highest electrical power. Energy, 2014;68:104–16.
[11] Sahin A, Yilbas, B. Thermodynamic irreversibility and performance characteristics of thermoelectric power generator. Energ. 2013; 55:899-904.
[12] Mavridou S, Mavropoulos G C, Bouris D, et al. Comparative design study of a diesel exhaust gas heat exchanger for truck applications with conventional and state of the art heat transfer enhancements. Applied Thermal Engineering, 2010, 30(8-9):935-947.
[13] Zhou Z G, Zhu D S, Wu H X, et al. Modeling, Experimental Study on the Heat Transfer Characteristics of Thermoelectric Generator. Journal of Thermal Science, 2013(01):48-54.

 